Lake Level Fluctuations in the Northern Great Basin for the Last 25,000 years

Lauren Santi[1], Alexandrea Arnold[1], Daniel E. Ibarra[2], Chloe Whicker[1], John Mering[1], Charles G. Oviatt[3], Aradhna Tripati[1]

[1]Department of Earth, Planetary, and Space Sciences, Department of Atmospheric and Oceanic Sciences, Institute of the Environment and Sustainability, Center for Diverse Leadership in Science, UCLA, Los Angeles, CA 90024

[2]Department of Geological Sciences, Stanford University, Stanford, CA, 94305

[3]Department of Geology, Kansas State University, Manhattan, Kansas, 66506

Corresponding authors: Lauren Santi (lsanti@ucla.edu), Alexandrea Arnold (ajarnold1@ucla.edu), Daniel Ibarra (danieli@stanford.edu), and Aradhna Tripati (atripati@g.ucla.edu)

This paper is a post print submitted to *EarthArXiv* and was published in *Exploring Ends of Eras in the eastern Mojave Desert* (editor D.M. Miller) 2019 Desert Symposium Field Guide and Proceedings, pages 176-186. (http://www.desertsymposium.org/About.html)

Lake Level Fluctuations in the Northern Great Basin for the Last 25,000 years

Lauren Santi[1], Alexandrea Arnold[1], Daniel E. Ibarra[2], Chloe Whicker[1], John Mering[1], Charles G. Oviatt[3], Aradhna Tripati[1]

[1]Department of Earth, Planetary, and Space Sciences, Department of Atmospheric and Oceanic Sciences, Institute of the Environment and Sustainability, Center for Diverse Leadership in Science, UCLA, Los Angeles, CA 90024

[2]Department of Geological Sciences, Stanford University, Stanford, CA, 94305

[3]Department of Geology, Kansas State University, Manhattan, Kansas, 66506

Abstract

During the Last Glacial Maximum (LGM; ~23,000 to 19,000 years ago or ka) and through the last deglaciation, the Great Basin physiographic region in the western United States was marked by multiple extensive lake systems, as recorded by proxy evidence and lake sediments. However, temporal constraints on the growth, desiccation, and timing of lake highstands remain poorly constrained. Studies aimed at disentangling hydroclimate dynamics have offered multiple hypotheses to explain the growth of post-LGM lakes; however, a more robust understanding is currently impeded by a general paucity of spatially and temporally robust data. In this study, we present new data constraining the timing and extent of lake highstands at three post-LGM age pluvial lakes: Lake Newark, Lake Surprise, and Lake Franklin. This data is used in concert with previously published data for these basins and others from the Northern Great Basin including Lakes Bonneville, Chewaucan, and Lahontan to compare the timings of lake growth and decay over a large spatial scale and constrain how regional hydroclimate evolved through the deglaciation.

Introduction

The American West is characterized by aridity and low precipitation, with many regions receiving under 250 mm of rain a year. Furthermore, this region is projected to become even drier in the coming years, though climate models used for forecasting these changes disagree in the magnitude of change in precipitation (Scheff and Frierson, 2012; Seager et al., 2010). One approach that can be used to improve our understanding of the role of different atmospheric processes in driving aridification in the West involves using paleoclimate data, as well as model-data comparisons, to study controls on past water balance.

In stark contrast to the present-day, during the Last Glacial Maximum (LGM; ~23 to 19 ka) and subsequent deglaciation (19 ka through ~11 ka, the onset of warming through the Younger Dryas and until the Holocene), the sedimentary record indicates the region was marked by >50 extensive lake systems (Hubbs and Miller, 1948; Mifflin and Wheat, 1979; Reheis, 1999; Reheis

et al., 2014; Ibarra et al., 2018; McGee et al., 2018). The predominance of late Pleistocene lakes in now-arid regions indicates significant changes in the water cycle in response to changing climate forcing. Water balance calculations indicate that precipitation increases up to 2 times modern, as well as reduced evaporation rates may be needed to explain the distribution of lakes at their greatest extent (e.g. Ibarra et al., 2014; Hudson et al., 2017; Ibarra et al., 2018; Ibarra et al., 2019). These calculations indicate that highstands (which largely occur after the LGM) cannot be singularly driven by low evaporation rates due to temperature depression associated with glacial periods. As such, there must be a significant contribution from precipitation driving these changes.

While the most recent iteration of global climate models (PMIP3) has produced precipitation estimates for an LGM simulation (21 ka), the next ensemble of simulations is the mid Holocene (6 ka) (Braconnot et al., 2012). This large gap in time makes it difficult to tease apart temporal variations in atmospheric dynamics that may be contributing to lake growth, only one model has been used for transient simulations (Transient Climate Evolution 'TraCE', run through the National Center for Atmospheric Research Community Climate System Model Version 3 'CCSM3'). Comparison of current these precipitation simulations show a general lack of agreement, indicating the atmospheric dynamics delivering precipitation to the region are not yet well understood (Figure 1).

One set of constraints on the mechanism(s) driving changes in hydroclimates comes from studies that have dated both carbonates and subaerial deposits (e.g., organic matter in soils) from paleoshorelines. These chronologies can be used to provide insights into potential mechanisms driving lake growth, including changes in precipitation. Recent work indicates non-synchronous lake highstands across the Great Basin, with some studies suggesting a latitudinal trend in the timing of maximum lake extent (Lyle et al., 2012; Munroe and Laabs, 2013a; Ibarra et al., 2014; Oster et al., 2015; Egger et al., 2018; McGee et al., 2018) that are not yet resolved with existing models. However, at present, the temporal and spatial evolution of lake highstands and stillstands is not chronologically constrained well enough to allow for meaningful insight into the atmospheric dynamics driving these changes, and therefore that is the focus of this work.

For this study, we collected tufa and gastropods shells from paleolake shorelines, including Lake Surprise, Lake Newark, and Lake Franklin (Figure 2), and determined elevation-age histories using radiometric dating based on carbon-14 analysis. We use our radiocarbon ages and previously published work to constrain lake hydrographs and also estimate a pluvial hydrologic index for each lake to further constrain past hydroclimate change.

Materials and Methods

Sample Collection

Samples consisted of both tufa and gastropod shells, which were collected from the shorelines of three closed basin paleolakes within the northern Great Basin in the western United States. These shorelines were identified through a combination of literature review (e.g., Reheis, 1999; Mifflin and Wheat, 1979; Hubbs and Miller, 1948), and Google Earth observations. At each site, care was made to ensure that all tufa and shells were *in situ*. In many cases, this necessitated digging pits ~1 meter into the ground using shovels and/or augers (following Munroe and Laabs, 2013). Post-excavation, the GPS coordinates of each sample were recorded, and the elevation of each sample was determined using the USGS Elevation Point Query Service, which reports ⅓ arc-second elevation data across the continental United States with an elevation resolution of ~4 meters. For a subset of lake basins (Lake Chewaucan, and most tufa from Lake Surprise), LIDAR elevation datasets are available from previous publications, which provide a much more precise elevation estimate (cf. Ibarra et al., 2014; Egger et al., 2018).

Sample Preparation

Samples (tufa and gastropod shells) were first rinsed by hand in deionized water (DI) to remove loosely-held secondary material. If deemed necessary, they were sonicated in room temperature DI for up to 30 minutes to remove loosely held contaminants and particles on the sample surface. For shells with delicate internal chambers, a small pick or tweezers were used to carefully scrape away internal pieces of sand or secondary carbonate.

For tufa collection, small handheld drills were sometimes necessary to remove carbonate from a host rock (e.g., Ibarra et al., 2014). To prevent potential bond reordering due to frictional heating, the drill speed during this process was limited in both duration and in speed. The resulting powder from this drilling process was ground using a mortar and pestle until the sample was a homogenous texture.

After creating a fine carbonate powder from each sample, a small amount of 3% H_2O_2 was added to each sample and left to react at room temperature for 1-4 hours. This process is commonly used to remove organic material (e.g Mering, 2015; Tripati et al., 2010; Suarez and Passey, 2014). Post-reaction with H_2O_2, all samples were dried in an oven set below 50°C, and placed in a desiccator for long-term storage (Tripati et al., 2010; Suarez and Passey, 2014; Defliese et al., 2015).

Radiocarbon Dating

Carbonate samples consist of tufa and gastropod shells. Age control was provided by radiocarbon dating. In this study, radiocarbon dating was completed via Accelerator Mass Spectrometry (AMS) at UC Irvine. The uncertainty associated with AMS ages was on the order of hundreds of years (Table 1). Note that several tufas were previously collected by Ibarra et al.

(2014) and dated using uranium-series methods (see note in Table 1). For all radiocarbon results (this study and others), we use *IntCal13* to convert conventional ^{14}C ages to calibrated ^{14}C ages, expressed as thousands of years before present, "ka" (Stuvier et al., 2019). Reservoir corrections for *IntCal13* are made using the procedure outlined in Stuiver and Polach (1977), which uses independent age estimates to constrain correction magnitudes during each time interval. We plot the median calibrated probability and the 2σ uncertainty.

Hydrologic Index (HI)

The "pluvial hydrologic index" is a physical basin parameter that describes the ratio of lake surface area to tributary area. Historically, it has been used as a means to determine the partitioning of rainfall into runoff and evaporation and otherwise approximating past hydroclimate assuming minimal change in drainage area and hypsometric curvature (e.g., Mifflin and Wheat, 1979; Reheis, 1999; Ibarra et al., 2014). We calculate the HI of each basin as a function of sample elevation (z) using hypsometric curves for each lake basin from the HydroSHEDS/HydroBASINS datasets (Lehner et al., 2008; Lehner and Grill, 2013; Messager et al., 2016) using Equation 1:

$$HI(z) = \frac{Lake\ Area(z)}{Lake\ Basin\ Area - Lake\ Area(z)} \qquad \text{Equation 1}$$

For the elevations added to the literature in this study, we use elevations pinned to a United States Geological Survey Digital 30 m Elevation Model.

Elevation Control

For each of the smaller lake basins analyzed (Chewaucan, Franklin, Newark, and Surprise), differential isostatic rebound is not taken into consideration for recorded GPS elevations. However, differential post-lacustrine isostatic rebound of up to 74 m is a known complicating factor at Lake Bonneville (e.g. Oviatt et al., 1992). For Lake Bonneville, most modern elevations plotted are translated to estimates of pre-rebound elevation using a linear model described in Oviatt et al. (1992). We use isostatically adjusted lake areas calculated by Adams and Bills (2016). For Lake Lahontan, similar simple elevation correction models are not available, thus we do not correct for isostatic rebound, though it may be as much as ~22 m (Adams et al., 1999).

Results

We compile existing age control that defines hydrographs for a subset of northern Great Basin pluvial lakes with new data from Lake Franklin, Newark, and Surprise (Figure 3). We overlay schematics of implied paleo-lake histories for each basin that have been created based on existing data compilations and alternative schematics for Lakes Franklin, Newark, and Surprise, in light of new data from this study. In order to assess spatial gradients in moisture balance, we

also plot HI again basin-center latitude and longitude in Figure 4. We discuss the results in order of geographic position of basin, beginning with the southernmost basin.

Lake Newark

Pluvial Lake Newark (39.5°N, 115.7°W) was located in east-central Nevada. Kurth et al. (2011) provides eight radiocarbon ages of ancient shorelines and an estimated lake highstand 16.4 ± 0.3 ka, which is roughly coincident with that of nearby Lake Franklin (Redwine, 2003; Kurth et al., 2011). LGM levels were generally moderate, with a sharp increase in lake level during the deglacial at ~16.7 ka followed by rapid decline to low levels. In this work, we provide two additional radiocarbon ages that increases the total range in paleolake elevations from previous studies and constrain moderate lake levels during the LGM and near desiccation by ~11 ka.

Lake Lahontan

Lake Lahontan (38.75–40.75°N, 117.5–120.5°W) was a spatially extensive lake system that, at its maximum extent, covered over 22,000 km^2 throughout northwestern Nevada, northeastern California, and southern Oregon (Russell, 1885). Lake Lahontan reached its highstand at 15.7 ± 0.3 ka (Adams and Wesnouwsky, 1998). This basin (and its associated subbasins) have been studied extensively, with radiocarbon dates from both lacustrine and subaerial carbonate materials (Adams, 1998; Benson et al., 2013; Benson et al., 1995; Hostetler & Benson, 1990; Petryshyn et al., 2016). Existing age control was compiled from Benson et al. (2013) and Adams et al. (2008) and schematic lake level curves after those references (as well as Reheis et al. (2014)) are overlaid on Figure 3c. During the LGM and early deglacial period, Lake Lahontan had a consistent shoreline at 1256 m (although there is a ~40 m spread amongst elevations). At ~17.8 ka, Lake Lahontan transgressed to a highstand of 1330 m, where is remained until ~14.1 ka. Although its regression is not as well constrained, there is indication of a fast decline in lake levels to 1206 m by 13.25 ka.

Lake Franklin

Lake Franklin (40.2°N, 115.3°W) was located in northeast Nevada, on the east side of the Ruby Mountains. This paleolake has a well-constrained hydrologic history. With a pre-LGM shoreline elevation of 1823 m, lake transgression started slowly in the late LGM, accelerated ~17.3 ka, and culminated in a lake highstand of 1850 m at ~17 ka. This highstand was followed by a regression to 1820 m by 14 ka (Munroe and Laabs 2013a; Munroe and Laabs 2013b). In this study, we present 12 new dates derived from gastropod shells to further refine the lake hydrograph. We modify an existing lake level curve from Munroe and Laabs (2013a) and overlay it on Figure 3. Two high elevation samples, collected from a lagoonal marsh in Lillquist (1994), are not included in the lake level curve (but are plotted on the hydrograph), as these likely represent an overestimate of lake extent (see discussion in Munroe and Laabs, 2013a). While not significantly extending the temporal range of data, our dates lie well within previously published values on the

lake hydrograph, and thus support the previously constructed lake level history by Munroe and Laabs (2013a).

Lake Bonneville

At its greatest extent, Lake Bonneville (38.5–43.5°N, 111.5–114.5°W) extended via multiple subbasins throughout central and northwest Utah, and into northeastern Nevada and southern Idaho. Lake Bonneville was comprised of the Bonneville Basin and the Sevier Subbasin, and contains the modern Great Salt Lake. This basin was spatially extensive (over 50,000 km^2), and has been studied in-depth in many publications since the original work by G.K. Gilbert (1890), including several recent studies constraining and compiling the lake hydrograph by Oviatt (2015), Reheis et al. (2014), McGee et al. (2012), Mering (2015) and Adams (2008). Existing radiocarbon ages analyzed here come from both lacustrine and terrestrial proxies, and have been delineated as such in Figure 3. The existing lake level curve indicates a gradual rise in lake levels prior to the LGM, with a potentially rapid transgression at ~19 ka. The maximum lake level attained at Lake Bonneville persisted between ~19-15 ka; however, as Lake Bonneville was not a closed basin during this period of time, this lake level is not representative of a true hydraulic maximum (Oviatt, 2015). After this period, Lake Bonneville stabilized at several lower-elevation shorelines, which have been denoted on Figure 2. We show a simplified lake level curve after Oviatt (2015) with ages from all the above-mentioned studies and compilations.

Lake Surprise

Lake Surprise (41.5°N, 120°W) was located on the border of northeast California and northwest Nevada. The geology and pluvial history of Lake Surprise was originally studied in Ibarra et al. (2014) and Egger et al. (2018). The current lake curve indicates a gradual increase in lake levels throughout the LGM and early deglacial period, culminating in a rapid rise occurring in less than 1 ka. Ibarra et al. (2014) first dated the post-LGM highstand at ~15.2 ka, and finds evidence of a maximum lake extent 176 meters above modern. In more recent work, Egger et al. (2018) added 12 radiocarbon dates to an existing repository of 21 dated samples, including a new higher elevation highstand age of ~16.0 ka. This rapid rise in lake levels is followed by a slow decline over the next 5 kyrs. In this work, we sought to fill in ages from moderate to high post-LGM but pre-highstand elevations, including new ages from the southernmost subbasin of Surprise Valley (Duck Flat). These ages compliment previously recorded ages at Lake Surprise by Ibarra et al. (2014) and Egger et al. (2018), but provide more detail by filling in missing gaps during the deglacial, including four tufa samples dated within ~2 ka of the highstand.

Lake Chewaucan

Chewaucan Lake (42.7°N, 120.5°W) was located in southern Oregon, and was comprised of four subbasins: Summer Lake, Upper Chewaucan Marsh, Lower Chewaucan Marsh, and Albert Lake. Albert Lake and Summer Lake are modern perennial lakes that become desiccated during the mid to late summer each year, and at times completely dry up. In the past, these subbasins had

variable connectivity, depending on the lake levels. Previously reconstructed shorelines (with most data deriving from Summer Lake) are compiled to produce a lake level curve for Lake Chewaucan (Hudson et al., 2017; Egger et al., 2018; Licciardi, 2001). There are two potential lake level trajectories for pre-LGM Lake Chewaucan, but both indicate a decrease in lake levels between 25-20 ka. Following an initial rise in lake levels, there is short desiccation at ~16 ka, prior to the highstand at 14-13 ka, where the lake reached 1356 m. Lake regression began ~13 ka, and continued throughout the remainder of the deglacial and into the early Holocene.

Discussion

1. Timing of high stands and lake level fluctuations

Lake Newark

Although the data is sparse, there is evidence that paleolake levels increased sharply at Lake Newark ~16.9 ka (Kurth et al., 2011). Two new radiocarbon dates from our study increase the temporal range of data, and indicate moderate lake levels prior to the LGM, as well as a continued decrease in lake extent during the late deglacial period.

Lake Lahontan

Data from Lake Lahontan encompasses both subaerial and lacustrine carbonates, with subaerial carbonates providing maximum lake extents, and most of these carbonates lying at higher elevations than the lacustrine carbonates within a similar time frame, as expected. The hydrologic history of Lake Lahontan is one of the best-constrained, due to numerous studies contributing hundreds of lacustrine carbonate and subaerial measurements. The lake level history is overlaid on Figure 3, and indicates a rapid rise from ~1260 m after the LGM at ~17.8 ka, to a highstand at ~1328 m, before an eventual regression around 14.5 ka (Benson et al., 1995; 2013; Benson, 2008; Adams et al., 2008).

Lake Franklin

New radiocarbon ages from Lake Franklin (this study) support the timing of the maximum lake extent documented by Munroe and Laabs (2013a), who put together the first cohesive lake history using new radiocarbon data along with existing data from Lillquist (1994). The oldest radiocarbon date provides evidence that Lake Franklin may have once stood above 1850 m, indicating that an overall highstand for Lake Franklin was prior to the LGM, in contrast to neighboring pluvial lakes (Munroe and Laabs, 2013a). However, Munroe and Laabs (2013a) note that this sample (an assemblage of shells) may have been taken from the wrong stratigraphic unit, and for that reason, was not included in the hydrograph and is thus correspondingly marked with a question mark on Figure 3.

During the early LGM (22.5-20 ka), Lake Franklin stood at an elevation of ~1823 m. Radiocarbon ages reflecting anomalously high lake elevations in this time period (~1850 m) are taken from lagoonal deposits (Lillquist, 1992), and likely reflect a near-shore environment above the main body of the lake. These are also set apart with question marks, and not used to construct the hydrograph itself (following Munroe and Laabs, 2013a).

Continuing to the late LGM, Lake Franklin rapidly grew to ~1830 m, where it remained relatively stable. There are two data points from this period that are outliers: one at 1840 m and one at 1823 m. These were excluded from the hydrograph because there is some uncertainty regarding their exact GPS location and stratigraphic context (see discussion in Munroe and Laabs, 2013a).

Between 16.8-17.3 ka, Lake Franklin rose from 1830 to its highstand elevation of 1850 m, indicating a ~168% lake area increase. Munroe and Laabs (2013a) argue for a rapid and temporary regression during this time period, before returning again to 1850 m.

Following the pluvial maximum, the lake stabilized at 1843 m, and then 1840 m, with multiple radiocarbon ages from each beach ridge indicating that lake levels may have stabilized at both locations more than once. Overall, the new data from this study fits in well with the lake hydrograph trajectory described by Munroe and Laabs (2013a), with a rapid transgression to the post-LGM highstand, followed by shorelines that stabilized at 1843 m and 1840 m.

Lake Bonneville

Lake Bonneville is one of the most studied paleolakes in the Great Basin to date, with over 300 radiocarbon ages from lacustrine and subaerial carbonate and organic matter through the last deglacial (e.g. Benson et al., 2011; Broecker and Kaufman 1965; Broecker and Orr 1958; Godsey et al., 2005; Mering, 2015; Nishizawa et al., 2013; Oviatt et al., 2005; Oviatt, 2015; Reheis et al., 2014). Due to Bonneville's great spatial extent and depth, measurements of lake shorelines are approximately corrected for the effects of differential isostatic rebound that vary between different subbasins, with the greatest rebound in the center of the basin (Adams and Bills, 2016). However, the reconstructed lake level history still shows a remarkably coherent story of lake level transgression and regression (Oviatt, 2015; Reheis et al., 2014).

Previously-defined lake level histories for Lake Bonneville have identified key events in the evolution of the lake. The initial rise of Lake Bonneville was quite rapid, potentially due to a diversion of the Upper Bear River, although there are other possible mechanisms, including a diversion from Cache Valley into the Great Salt Lake basin (Reheis et al., 2014). The lake reached its highstand at 18.6 ± 0.14 ka (McGee et al, 2012; Oviatt, 2015) where its maximum elevation was limited by intermittent overflow. This overflow limited its maximum pluvial extent, and is thus a key constraint for reconstructions of lake history. Putting a dramatic end to

this highstand, Lake Bonneville catastrophically flooded to the nearby Snake River basin prior to ~18.2 ka (potentially much sooner, after rising to an overflow point near Red Rock Pass), and the shoreline transgressed to the new, "Provo Shoreline" level, where it remained for several thousand years (Godsey et al., 2005). The lake subsided rapidly from the Provo shoreline, and ceased to overflow, at about 15 ka (Godsey et al., 2011). With continued regression following the Provo Shoreline time, Lake Bonneville split into separate lakes, with Lake Gunnison persisting in the interior of the Sevier subbasin until ~10 ka, and the Gilbert-episode lake (a brief rise ~11.5 ka) encompassing the modern Great Salt Lake (but ~15 m higher) and extending to its west (Oviatt, 2014).

Samples at Lake Bonneville define a lake level "envelope", with subaerial samples indicating a maximum lake elevation, and lacustrine samples indicating a minimum lake elevation. Subaerial samples define a consistent maximum lake elevation between ~18-20 ka, but are intermixed with lacustrine carbonates during other time periods (e.g., 27-23 ka and 18.0-15.0 ka). This inconsistency could be explained by radiocarbon reservoirs within ancient Lake Bonneville; however, many existing studies suggest that this effect is relatively small (Currey and Oviatt, 1985; Godsey, 2005; McGee et al., 2012). For example, McGee et al. (2012) show concordant radiocarbon and U-Th ages from Cathedral Cave in the main body of Lake Bonneville. Furthermore, Benson et al. (2011) show good correspondence between dates derived from a paleomagnetic secular variation model and radiocarbon ages from a sediment core taken from the western edge of the basin.

However, some caution should be taken when interpreting radiocarbon ages when concurrent dating methods are not used. Concurrence between dating methods at a single location does not guarantee it can be extrapolated throughout the entire basin. For example, one area within ancient Lake Bonneville, Tabernacle Hill, is a site of current hot springs, high water tables, and tufa mounds dating to pre-Bonneville times, all of which indicate that groundwater could have provided a source of carbon for the Provo Lake. Ultimately, there is no indication of a major radiocarbon reservoir, but interpretation of radiocarbon ages should still consider this potential source of uncertainty.

Lake Surprise

Additional radiocarbon dates from pluvial Lake Surprise (this study) largely support the trend in lake levels indicated by previous work (Ibarra et al., 2014; Egger et al., 2018). New data from ~20 to 24 ka compare favorably with existing data, whilst filling in some temporal gaps at 20 ka. Similarly, new data collected just prior to the lake highstand at 15.2 ka is consistent with previous lake histories, which suggest a rapid increase in lake levels prior to the highstand (Ibarra et al., 2014; Ibarra et al., 2018). Several radiocarbon dates from this study show low lake levels until as late as almost 16 ka, indicating that Lake Surprise transgressed to its highstand

more rapidly than constrained by previous work, possible suggesting a large and rapid precipitation forcing also observed at Lake Franklin and Lake Lahontan.

Lake Chewaucan

According to previous highstand estimates, Lake Chewaucan was the last studied lake to reach maximum levels during the deglacial, between 13-14 ka. As the most northwestern of the well-studied Great Basin lakes, the highstand is consistent with a northwest-trending change in moisture delivery.

Figure 3 shows two potential trajectories for the Lake Chewaucan prior to 25 ka, one at very high lake levels and the other at low levels. There are several explanations for the possible trajectories. For one, the Summer Subbasin sample locality (from which these older samples were collected) contains the most active faults of the region, so samples could potentially be displaced from their original elevations (see discussion in Egger et al., 2018; Liccardi, 2001). Second, as tufa defines a minimum (but not absolute) shoreline, there is a chance that both sets of elevations could be correct, but the samples <1340 m formed deeper underwater. However, we view this explanation as unlikely; as tufa formation requires sunlight, its formation is limited to the photic zone near the lake surface. Additionally, prior to the ultimate highstand elevation, there is the possibility of a slight desiccation of the lake around 17 ka. This is similar to observations made at Lake Surprise (see below; Egger et al., 2018), but not to the same magnitude.

Summary of Lake Level Histories

Overall, we observe non-synchronicity in the timing of lake highstands, progressing from the southeast to the northwest during the deglacial period. In many cases, lake transgressions to their highstand levels (from moderate stillstand levels) happened in a relatively short period of time between 17 and 14 ka, while transgressions tended to occur over a much longer period. New data from this study provides higher temporal resolution for hydrographs, and in some cases, extends the timeline of hydrographs.

2. Spatial Variability in Hydrologic Indices

The hydrologic index (HI) is a useful indicator for past water balance because it normalizes changes in lake elevation to basin area, such that proportional changes can be directly compared between basins. Assuming minimal changes in groundwater storage or inputs, the HI can be directly related to the mass balance of the watershed (see application in Mifflin and Wheat, 1979; Reheis, 1999; Ibarra et al., 2014; 2018). Additionally, when plotting HI versus latitude or longitude, trends may indicate latitudinal or longitudinal gradients in catchment-scale moisture balance. All sites except Lake Bonneville show an increase in HI following the LGM. Lake

Bonneville, because it was an overflowing lake after the LGM (Oviatt, 2015), did not record meaningful HI for the deglacial.

The latitudinal gradient in HI (Fig. 4) shows a significant increase in maximum deglacial HI with latitude, with a maximum HI of 0.530 attained by Lake Chewaucan. The longitudinal trend in HI shows a dipole, with lower values between 115°W and 120°W (roughly coincident with the eastern and western borders of Nevada). Lakes in the west and east have contributing watersheds that include the high-altitude Sierra Nevada and Uinta Mountains, which may account for part of this pattern. Here we primarily focus on a longitudinal spread (111°W to 121°W) of lakes with minimal latitudinal variation (38°N to 43°N), at present further work is needed in the southern Great Basin to more robustly constrain latitudinal trends.

Overall, the lower-latitude sites with a longitude between 115°W and 120°W experience the smallest change in HI during the deglacial. This is likely not biased due to low sampling resolution, as the lake basins from the two smallest HI's (corresponding to Lakes Franklin and Lahontan), have a significant amount of data, and demonstrate well-defined shorelines and hydrographs. The fine scale trends in moisture gradients inferred from HI values could be consistent with vapor transport by atmospheric rivers (Lora et al., 2016), or other transport mechanisms (e.g., McGee et al., 2018), though further work on the numerous pluvial lakes in the Great Basin will be needed for this hypothesis to be tested.

Conclusions

Constraining the timing of lake highstands has important implications for understanding the terrestrial and atmospheric processes that transport moisture and impart changes on the basin-scale hydrological cycle. Post-LGM lake highstands at Great Basin pluvial lakes have previously shown non-synchronicity, with lake highstands progressing from the southeast to the northwest during the deglacial period (McGee et al., 2018). This study adds 22 additional carbonate ages to the existing repository of data, and synthesizes and compares this to existing data from the literature. Overall, new data largely supports previously noted temporal trends in lake highstands, with the most recent highstands occurring in the northwestern lake basins.

New data from this study provide additional insight into previously compiled lake hydrographs. For example, radiocarbon ages from Lake Surprise provide more precise constraints on the timing of the lake highstand, and support a fast transgression at ~16 ka, suggesting a large precipitation forcing. Additionally, new ages from Lake Newark expand the temporal range of data, and provide a better idea of pre-LGM lake levels. Finally, new data from Lake Franklin and Lake Surprise fill in temporal gaps in existing data, and largely support previously constructed lake hydrographs.

Ultimately, our analysis of pluvial hydrologic index (HI) with latitude and longitude reveals systematic spatial trends that will provide targets for future climate modeling efforts. The highest post-LGM HI values are found at high latitudes, and either west of 120°W, or east of 115°W. Given further work, this spatial variability in HI could be used to robustly infer temporal and spatial changes in atmospheric moisture sources, and will provide targets for future transient simulations of the deglaciation.

Figures:

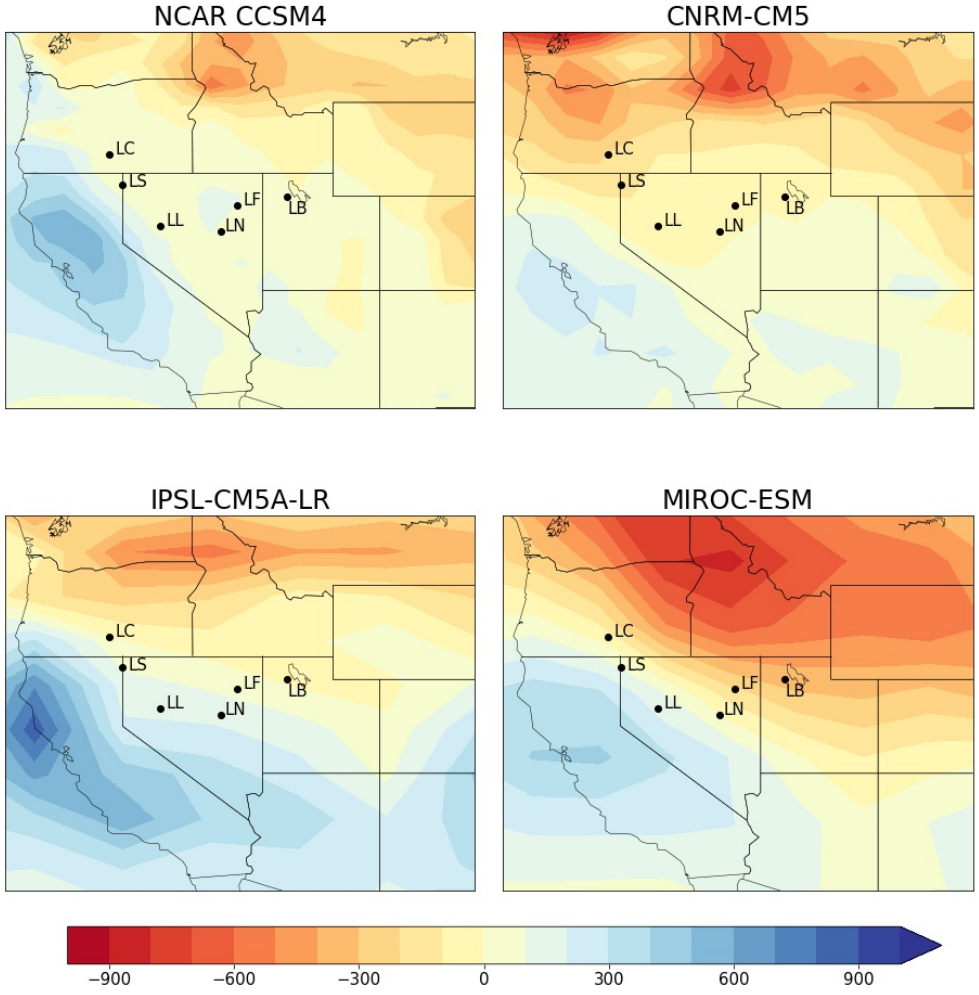

Figure 1: PMIP3-derived precipitation anomaly maps of the western United States from individual simulations. The annual precipitation anomaly is calculated as LGM minus preindustrial simulation, in mm/year. The LGM simulation is set to 21 ka, while the preindustrial simulation represents "0 ka". Note that both the spatial patterns of precipitation and the color bars are not the same scale. No bias correction was applied and all maps were made using the original resolution of the climate model outputs. The centroids of watershed polygons discussed in this study are plotted for reference. Model output is from the World Climate Research Programme's Coupled Model Intercomparison Project phase 5 (CMIP5) multi-model dataset. Labels = Lake Surprise (LS), Lake Newark (NL) and Lake Franklin (LF). Other lakes include: Lake Bonneville (LB), Lake Lahontan (LL), and Lake Chewaucan (LC).

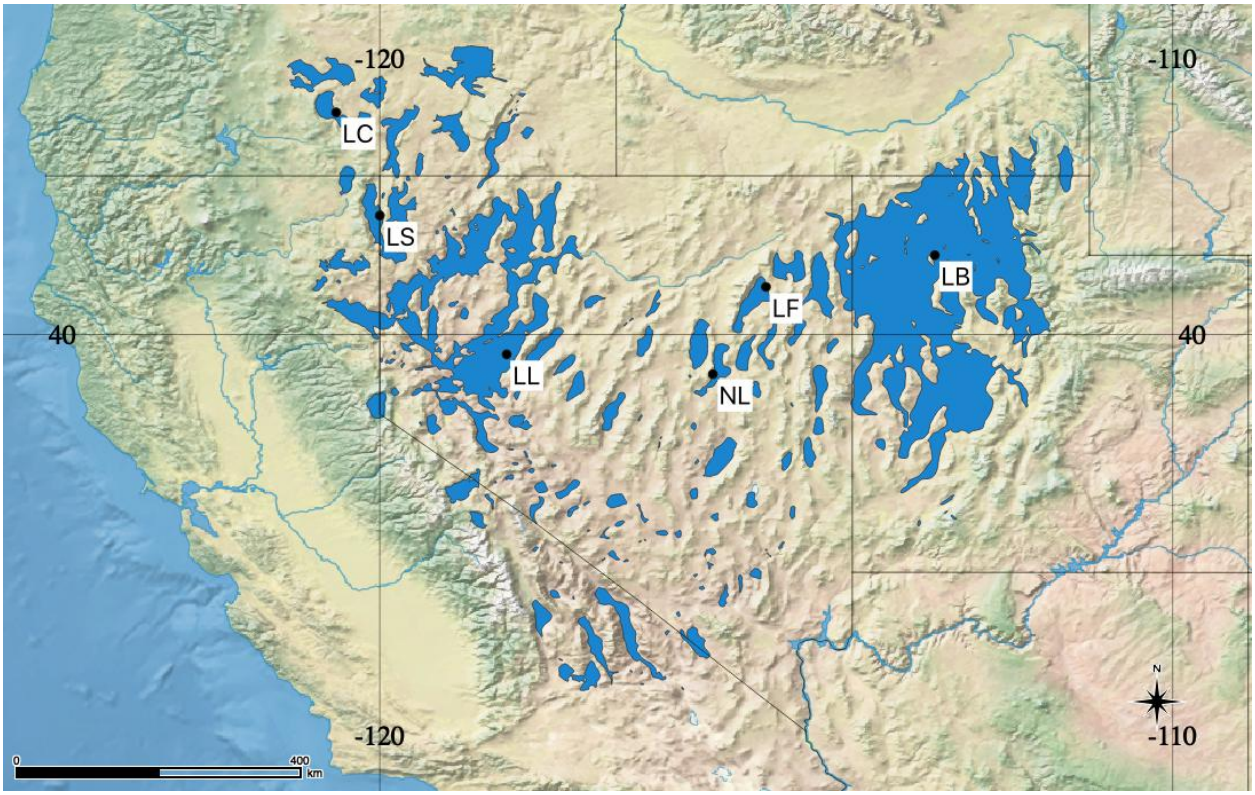

Figure 2: Pluvial lakes included in this study or plotted in Figure 3. New ages are from: Lake Surprise (LS), Lake Newark (NL) and Lake Franklin (LF). Other lakes include: Lake Bonneville (LB), Lake Lahontan (LL), and Lake Chewaucan (LC). Blue area is maximum pluvial lake extent during the LGM and deglacial, digitized from Mifflin and Wheat (1979) estimates (Map made using *Natural Earth* physical vector data).

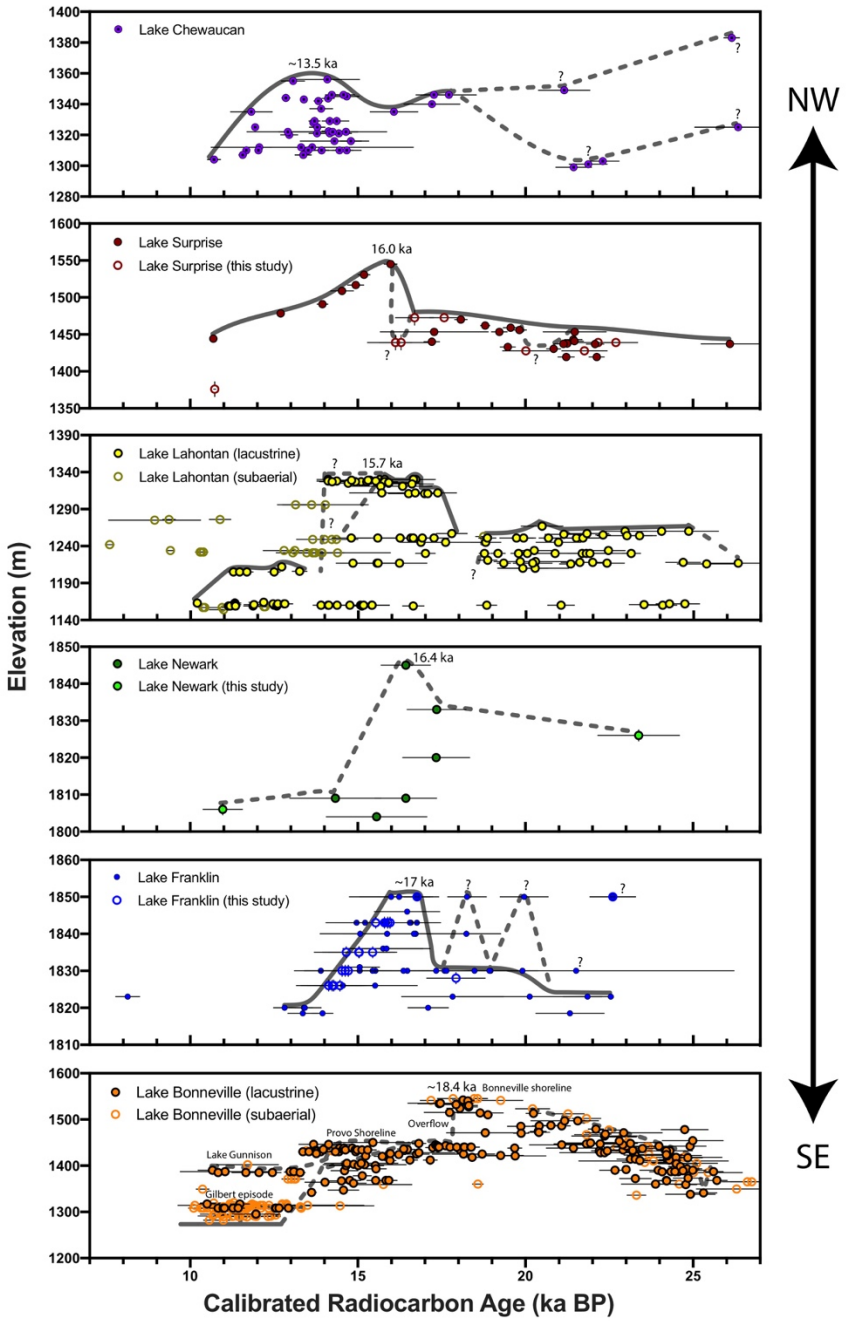

Figure 3: Radiocarbon based lake hydrographs for northern Great Basin pluvial lakes. Basins are plotted from geographic northwest to southeast. Lake Bonneville and Lake Lahontan data define lake elevation envelopes (see Oviatt, 2015; Benson et al., 2013; Adams et al., 2008), with terrestrial materials delineating a maximum lake extent, and lacustrine materials indicating a minimum lake extent. Projected lake level histories are overlaid on each basin. Some of these lake level histories have been altered from previous publications based on new data from this study. Errors in calibrated radiocarbon ages represent 2σ uncertainties and elevation errors are the same as originally reported for previous data, and are $\pm$1.5m for this study. Chewaucan data after Egger et al., (2018) and Liccardi (2001), Lake Lahontan data after Benson et al., (2013) and Adams et al., (2008), Lake Franklin data after Munroe and Laabs (2013), Lake Surprise data after Ibarra et al. (2014) and Egger et al. (2018), and Lake Bonneville data after Oviatt et al., 2015 and Mering, 2015.

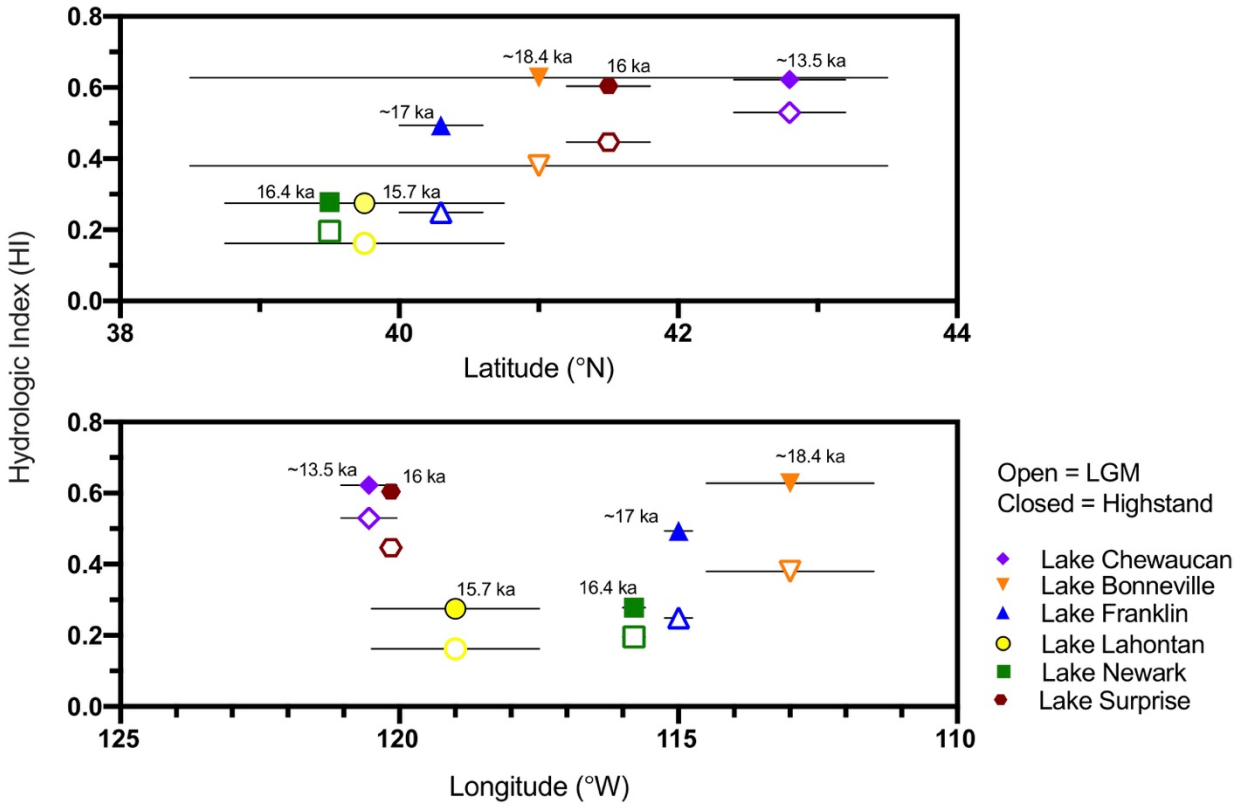

Figure 4: Hydrologic Indices (HI) plotted as a function of basin-center latitude (a) and longitude (b). Filled shapes indicate the maximum HI during the LGM (19-23 ka), while clear shapes indicate the maximum HI during the LGM and the deglacial intervals Estimated timing of each highstand is indicated. HI values are reported in Supplementary Materials Table 2. Horizontal bars indicate the maximum geographic span of the lake.

Tables:

Table 1: New Radiocarbon Ages for Northern Great Basin Pluvial Lakes

Lake Basin	Sample Name	Sample Type	GPS Location	^{14}C Age	^{14}C Age	IntCal13 Age (ka)	2σ min	2σ max	Elevation (m)	HI
Franklin	FranklinRW1_60_1A	Gastropod shell	40,6472N; -115,1388W	12.260	0.11(	14.233	13.821	14.765	1826	0.21
Franklin	FranklinRW1_60_2A	Gastropod shell	40.1832N; -115.3760W	12.370	0.12(	14.466	14.044	15.020	1826	0.21
Franklin	FranklinRW1_60_2B	Gastropod shell	40.1832N; -115.3760W	12.200	0.13(	14.127	13.752	14.715	1826	0.21
Franklin	FranklinRW2_90_1A	Gastropod shell	40.2813N; -115.3760W	12.520	0.19(	14.713	14.041	15.339	1838	0.36
Franklin	FranklinRW2_90_1B	Gastropod shell	40.2813N; -115.3760W	12.400	0.16(	14.530	13.999	15.133	1838	0.36
Franklin	FranklinRW3_78_1A	Gastropod shell	40.2809N; -115.3601W	12.480	0.12(	14.654	14.163	15.122	1841	0.39
Franklin	FranklinRW3_78_1B	Gastropod shell	40.2809N; -115.3601W	12.910	0.12(	15.437	15.093	15.818	1841	0.39
Franklin	FranklinRW3_78_1C	Gastropod shell	40.2809N; -115.3601W	12.670	0.12(	15.027	14.377	15.454	1841	0.39
Franklin	FranklinFRB_170_1	Tufa	40.6472N; -115.1388W	14.730	0.18(	17.925	17.492	18.362	1848	0.48
Franklin	FranklinHS1_86_1A	Gastropod shell	40.2477N; -115.1388W	13.230	0.14(	15.891	15.408	16.277	1843	0.49
Franklin	FranklinHS186_1B	Gastropod shell	40.2477N; -115.1388W	12.980	0.16(	15.529	15.088	16.029	1843	0.49
Franklin	FranklinHS1_86_1C	Gastropod shell	40.2477N; -115.1388W	13.280	0.14(	15.960	15.493	16.361	1843	0.49
Newark	NewarkLmt3_185_1	Tufa	39.4776N; -115.7882W	19.420	0.25(	23.383	22.777	24.001	1826	0.196
Newark	NewarkLmt4_50_1	Tufa	39.4547N; -115.7790W	9.650	0.12(	10.973	10.658	11.253	1806	0.136
Surprise	SVDI12-T4A*	Tufa	41.4299N; -119.9752W	18.780	0.27(	22.697	22.039	23.354	1439	0.332
Surprise	SVDI12-T4B*	Tufa	41.4299N; -119.9752W	18.350	0.27(	22.181	21.532	22.807	1439	0.332
Surprise	SVDI12-T7*	Tufa	41.4280N; -119.9725W	14.460	0.17(	17.613	17.141	18.008	1472.5	0.424
Surprise	SVDI12-T3A*	Tufa	41.4299N; -119.9752W	18.030	0.28(	21.823	21.083	22.443	1427.8	0.306
Surprise	SVDI12-T3B*	Tufa	41.4299N; -119.9752W	16.590	0.29(	20.016	19.279	20.713	1427.8	0.306
Surprise	SVCW17-PT1	Tufa	40.9771N; -119.8755W	13.520	0.34(	16.303	15.289	17.288	1475	0.444
Surprise	SVCW17-PT2	Tufa	40.9770N; -119.8755W	13.390	0.16(	16.109	15.642	16.609	1475	0.444
Surprise	SVCW17-PT3	Tufa	40.9764N; -119.8747W	13.790	0.19(	16.684	16.126	17.258	1477	0.445

*Originally collected and dated by uranium-series only in Ibarra et a. (2014)

Table 2: Calculated hydrologic indices for each basin

Pluvial Lake	LGM Maximum Hydrologic Index (19-23 ka)	Deglacial Highstand Hydrologic Index
Chewaucan	0.530	0.622
Surprise	0.447	0.604
Lahontan	0.162	0.275
Newark	0.196	0.278
Franklin	0.249	0.494
Bonneville	0.380	0.628[a]

[a] Bonneville shoreline prior to spillover at ~18 ka

Acknowledgements

This work and all UCLA participants were supported by an NSF CAREER award (NSF EAR-1352212) to Aradhna Tripati. Lauren Santi and Alexandrea Arnold received support from the Center for Diverse Leadership in Science, and Alexandrea Arnold was also supported by a Cota-Robles Fellowship. Kate Maher provided funding for Lake Surprise sample collection by Daniel Ibarra, Sarah Lummis, and Chloe Whicker, supported by the National Science Foundation (NSF) grant EAR-0921134. Daniel E. Ibarra is supported by a Heising-Simons Foundation grant to C. Page Chamberlain.

We acknowledge the modeling groups, the Program for Climate Model Diagnosis and Intercomparison (PCMDI) and the WCRP's Working Group on Coupled Modelling (WGCM) for their roles in making available the WCRP CMI53 multi-model dataset. Support of this dataset is provided by the Office of Science, U.S. Department of Energy.

References

Adams, K.D., and Bills, B.G. (2016), Chapter 8. Isostatic rebound and palinspastic restoration of the Bonneville and Provo shorelines in the Bonneville basin, UT, NV, and ID, in Oviatt, C.G.,Shroder Jr., J.F., editors, Lake Bonneville: A Scientific Update:Developments in Earth Surface Processes, Elsevier, v. 20. p. 145–164

Adams, K. D., Goebel, T., Graf, K., Smith, G. M., Camp, A. J., Briggs, R. W., & Rhode, D. (2008). Late Pleistocene and early Holocene lake-level fluctuations in the Lahontan Basin, Nevada: Implications for the distribution of archaeological sites. *Geoarchaeology*, *23*(5), 608-643.

Adams, K. D., & Wesnousky, S. G. (1998). Shoreline processes and the age of the Lake Lahontan highstand in the Jessup embayment, Nevada. *Geological Society of America Bulletin*, *110*(10), 1318-1332.

Adams, K. D., Wesnousky, S. G., & Bills, B. G. (1999). Isostatic rebound, active faulting, and potential geomorphic effects in the Lake Lahontan basin, Nevada and California. *Geological Society of America Bulletin*, *111*(12), 1739-1756.

Benson, L.V., Kashgarian, M., & Rubin, M. (1995). Carbonate deposition, Pyramid Lake subbasin, Nevada: 2. Lake levels and polar jet stream positions reconstructed from radiocarbon ages and elevations of carbonates (tufas) deposited in the Lahontan basin. *Palaeogeography, Palaeoclimatology, Palaeoecology*, *117*(1-2), 1-30.

Benson, L. V., Lund, S. P., Smoot, J. P., Rhode, D. E., Spencer, R. J., Verosub, K. L., ... & Negrini, R. M. (2011). The rise and fall of Lake Bonneville between 45 and 10.5 ka. *Quaternary International*, *235*(1-2), 57-69.

Benson, L. V., Smoot, J. P., Lund, S. P., Mensing, S. A., Foit Jr, F. F., & Rye, R. O. (2013). Insights from a synthesis of old and new climate-proxy data from the Pyramid and Winnemucca lake basins for the period 48 to 11.5 cal ka. *Quaternary International*, *310*, 62-82.

Braconnot, P., Harrison, S. P., Kageyama, M., Bartlein, P. J., Masson-Delmotte, V., Abe-Ouchi, A., Otto-Bleisner, B., & Zhao, Y. (2012). Evaluation of climate models using palaeoclimatic data. *Nature Climate Change*, *2*(6), 417.

Broecker, W. S., McGee, D., Adams, K. D., Cheng, H., Edwards, R. L., Oviatt, C. G., & Quade, J. (2009). A Great Basin-wide dry episode during the first half of the Mystery Interval?. *Quaternary Science Reviews*, *28*(25-26), 2557-2563.

Broecker, W. S., & Orr, P. C. (1958). Radiocarbon chronology of Lake Lahontan and Lake Bonneville. *Geological Society of America Bulletin*, *69*(8), 1009-1032.

Chiang, J. C., Lee, S. Y., Putnam, A. E., & Wang, X. (2014). South Pacific Split Jet, ITCZ shifts, and atmospheric North–South linkages during abrupt climate changes of the last glacial period. *Earth and Planetary Science Letters*, *406*, 233-246.

Defliese, W. F., Hren, M. T., & Lohmann, K. C. (2015). Compositional and temperature effects of phosphoric acid fractionation on Δ47 analysis and implications for discrepant calibrations. *Chemical Geology*, *396*, 51-60.

Egger A.E., Ibarra, D.E., Widden, R, Langridge R.M., Marion, M, & Hall, J. (2018). Influence of Pluvial Lake Cycles on Earthquake Recurrence on the Northwestern Basin and Range, USA. *Geological Society of America* Special Paper 536, 1-28.

Gilbert, G. K. (1890). *Lake Bonneville* (Vol. 1). US Government Printing Office, 1-438.

Godsey, H. S., Currey, D. R., & Chan, M. A. (2005). New evidence for an extended occupation of the Provo shoreline and implications for regional climate change, Pleistocene Lake Bonneville, Utah, USA. *Quaternary Research*, *63*(2), 212-223.

Godsey, H. S., Oviatt, C. G., Miller, D. M., & Chan, M. A. (2011). Stratigraphy and chronology of offshore to nearshore deposits associated with the Provo shoreline, Pleistocene Lake Bonneville, Utah. *Palaeogeography, Palaeoclimatology, Palaeoecology*, *310*(3-4), 442-450.

Hostetler, S., & Benson, L. V. (1990). Paleoclimatic implications of the high stand of Lake Lahontan derived from models of evaporation and lake level. *Climate dynamics*, *4*(3), 207-217.

Hubbs, C.L., and Miller, R.R. (1948). The zoological evidence: Correlation between fish distribution and hydro- graphic history in the desert basins of western United States, in The Great Basin with emphasis on glacial and postglacial times: *Bulletin of the University of Utah*, 38(20), 17–166.

Ibarra, D. E., Egger, A. E., Weaver, K. L., Harris, C. R., & Maher, K. (2014). Rise and fall of late Pleistocene pluvial lakes in response to reduced evaporation and precipitation: Evidence from Lake Surprise, California. *Bulletin*, *126*(11-12), 1387-1415.

Ibarra, D. E., Oster, J. L., Winnick, M. J., Caves Rugenstein, J. K., Byrne, M. P., & Chamberlain, C. P. (2018). Warm and cold wet states in the western United States during the Pliocene–Pleistocene. *Geology*, *46*(4), 355-358.

Ivanovic, R., Gregoire, L., Kageyama, M., Roche, D., Valdes, P., Burke, A., Drummond, R., Peltier, W & Tarasov, L. (2016). Transient climate simulations of the deglaciation 21-9 thousand years before present (version 1)-PMIP4 Core experiment design and boundary conditions. *Geoscientific Model Development*, 9(7), 2563-2587

Jayko, A. S., Forester, R. M., Kaufman, D. S., Phillips, F. M., Yount, J. C., McGeehin, J., ... & Miller, D. M. (2008). Late Pleistocene lakes and wetlands, Panamint Valley, Inyo County, California. *SPECIAL PAPERS-GEOLOGICAL SOCIETY OF AMERICA*, *439*, 151.

Jenkins, D. L., Davis, L. G., Stafford, T. W., Campos, P. F., Hockett, B., Jones, G. T., Yost, L., Connolly, T., Yohe, R., & Gibbons, S. C. (2012). Clovis age Western Stemmed projectile points and human coprolites at the Paisley Caves. *Science*, *337*(6091), 223-228.

Jones, M. D., Roberts, C. N., & Leng, M. J. (2007). Quantifying climatic change through the last glacial–interglacial transition based on lake isotope palaeohydrology from central Turkey. *Quaternary Research*, *67*(3), 463-473.

Kaufman, A., & Broecker, W. (1965). Comparison of Th230 and C14 ages for carbonate materials from Lakes Lahontan and Bonneville. *Journal of geophysical Research*, *70*(16), 4039-4054.

Kim, S. J., Crowley, T. J., Erickson, D. J., Govindasamy, B., Duffy, P. B., & Lee, B. Y. (2008). High-resolution climate simulation of the last glacial maximum. *Climate Dynamics*, *31*(1), 1-16.

Kurth, G., Phillips, F. M., Reheis, M. C., Redwine, J. L., & Paces, J. B. (2011). Cosmogenic nuclide and uranium-series dating of old, high shorelines in the western Great Basin, USA. *Bulletin*, *123*(3-4), 744-768.

Lehner, B., & Grill, G. (2013). Global river hydrography and network routing: baseline data and new approaches to study the world's large river systems. *Hydrological Processes*, *27*(15), 2171-2186.

Lehner, B., Verdin, K., and Jarvis, A. (2008). New Global Hydrography Derived From Spaceborne Elevation Data. *Eos, Transactions American Geophysical Union*, 89(10),93–94.

Licciardi, J. M. (2001). Chronology of latest Pleistocene lake-level fluctuations in the pluvial Lake Chewaucan basin, Oregon, USA. *Journal of Quaternary Science: Published for the Quaternary Research Association*, *16*(6), 545-553.

Lillquist, K. D. (1994). Late Quaternary Lake Franklin: lacustrine chronology, coastal geomorphology, and hydrostatic deflection in Ruby Valley and northern Butte Valley, Nevada. *Doctoral dissertation, PhD thesis, University of Utah, Salt Lake City, Utah*, 2618-2618.

Liu, Z., Otto-Bliesner, B. L., He, F., Brady, E. C., Tomas, R., Clark, P. U., ... & Erickson, D. (2009). Transient simulation of last deglaciation with a new mechanism for Bølling-Allerød warming. *Science*, *325*(5938), 310-314.

Lora, J. M., Mitchell, J. L., & Tripati, A. E. (2016). Abrupt reorganization of North Pacific and western North American climate during the last deglaciation. *Geophysical Research Letters*, *43*(22), 11-796.

Lyle, M., Heusser, L., Ravelo, C., Yamamoto, M., Barron, J., Diffenbaugh, N. S., ... & Andreasen, D. (2012). Out of the tropics: the Pacific, Great Basin Lakes, and Late Pleistocene water cycle in the western United States. *Science*, *337*(6102), 1629-1633.

Matsubara, Y., & Howard, A. D. (2009). A spatially explicit model of runoff, evaporation, and lake extent: Application to modern and late Pleistocene lakes in the Great Basin region, western United States. *Water Resources Research*, *45*(6), 1-18.

McGee, D., Moreno-Chamarro, E., Marshall, J., & Galbraith, E. D. (2018). Western US lake expansions during Heinrich stadials linked to Pacific Hadley circulation. *Science advances*, *4*(11), 1-10.

McGee, D., Quade, J., Edwards, R. L., Broecker, W. S., Cheng, H., Reiners, P. W., & Evenson, N. (2012). Lacustrine cave carbonates: Novel archives of paleohydrologic change in the Bonneville Basin (Utah, USA). *Earth and Planetary Science Letters*, *351*, 182-194.

Meehl, G. A., Covey, C., Delworth, T., Latif, M., McAvaney, B., Mitchell, J. F., Stouffer R., & Taylor, K. E. (2007). The WCRP CMIP3 multimodel dataset: A new era in climate change research. *Bulletin of the American Meteorological Society*, *88*(9), 1383-1394.

Mering, J. A. (2015). New constraints on water temperature at Lake Bonneville from carbonate clumped isotopes. *Doctoral dissertation, UCLA*. 1-178.

Messager, M.L., Lehner, B., Grill, G., Nedeva, I., and Schmitt, O. (2016). Estimating the volume and age of water stored in global lakes using a geo-statistical approach. *Nature Communications*, 7,13603.

Mifflin, M.D., and Wheat, M.M. (1979). Pluvial Lakes and Estimated Pluvial Climates of Nevada. *Nevada Bureau of Mines and Geology Bulletin,* 94, 1-57.

Miller, D. M., Oviatt, C. G., & Mcgeehin, J. P. (2013). Stratigraphy and chronology of Provo shoreline deposits and lake-level implications, Late Pleistocene Lake Bonneville, eastern Great Basin, USA. *Boreas*, *42*(2), 342-361.

Munroe, J. S., & Laabs, B. J. (2013). Latest Pleistocene history of pluvial Lake Franklin, northeastern Nevada, USA. *GSA Bulletin*, *125*(3-4), 322-342.

Munroe, J. S., & Laabs, B. J. (2013). Temporal correspondence between pluvial lake highstands in the southwestern US and Heinrich Event 1. *Journal of Quaternary Science*, *28*(1), 49-58.

Nishizawa, S., Currey, D. R., Brunelle, A., & Sack, D. (2013). Bonneville basin shoreline records of large lake intervals during Marine Isotope Stage 3 and the Last Glacial Maximum. *Palaeogeography, palaeoclimatology, palaeoecology*, *386*, 374-391.

Oster, J. L., Ibarra, D. E., Winnick, M. J., & Maher, K. (2015). Steering of westerly storms over western North America at the Last Glacial Maximum. *Nature Geoscience*, *8*(3), 201.

Oviatt, C. G., Currey, D. R., & Sack, D. (1992). Radiocarbon chronology of Lake Bonneville, eastern Great Basin, USA. *Palaeogeography, Palaeoclimatology, Palaeoecology*, *99*(3-4), 225-241.

Oviatt, C. G., & Jewell, P. W. (2016). The Bonneville shoreline: reconsidering Gilbert's interpretation. *In Developments in Earth Surface Processes,* 20, 88-104.

Oviatt, C. G. (2015). Chronology of Lake Bonneville, 30,000 to 10,000 yr BP. *Quaternary Science Reviews*, *110*, 166-171.

Petryshyn, V. A., Rivera, M. J., Agić, H., Frantz, C. M., Corsetti, F. A., & Tripati, A. E. (2016). Stromatolites in Walker Lake (Nevada, Great Basin, USA) record climate and lake level changes~ 35,000 years ago. *Palaeogeography, palaeoclimatology, palaeoecology*, *451*, 140-151.

Redwine, J. L. (2003). The Quaternary pluvial history and paleoclimate implications of Newark Valley, east-central Nevada, derived from mapping and interpretation of surficial units and geomorphic features. *Doctoral dissertation, Humboldt State University*, 1-385.

Reheis, M. (1999). Highest pluvial-lake shorelines and Pleistocene climate of the western Great Basin. *Quaternary Research*, *52*(2), 196-205.

Russell, I. C. (1885). *Geological history of Lake Lahontan: a Quaternary lake of northwestern Nevada* (Vol. 11). US Government Printing Office, 6.

Scheff, J., & Frierson, D. M. (2012). Robust future precipitation declines in CMIP5 largely reflect the poleward expansion of model subtropical dry zones. *Geophysical Research Letters*, *39*(18), 6p.

Seager, R., & Vecchi, G. A. (2010). Greenhouse warming and the 21st century hydroclimate of southwestern North America. *Proceedings of the National Academy of Sciences*, *107*(50), 21277-21282.

Stuiver, M., Pearson, G. W., & Braziunas, T. (1986). Radiocarbon age calibration of marine samples back to 9000 cal yr BP. *Radiocarbon*, *28*(2B), 980-1021.

Stuiver, M., & Polach, H. A. (1977). Discussion reporting of 14 C data. *Radiocarbon*, *19*(3), 355-363.

Stuiver, M., Reimer, P.J., and Reimer, R.W., 2019, CALIB 7.1 [WWW program] at http://calib.org, accessed 2019-2-10.

Suarez, M. B., & Passey, B. H. (2014). Assessment of the clumped isotope composition of fossil bone carbonate as a recorder of subsurface temperatures. *Geochimica et Cosmochimica Acta*, *140*, 142-159.

Tripati, A. K., Eagle, R. A., Thiagarajan, N., Gagnon, A. C., Bauch, H., Halloran, P. R., & Eiler, J. M. (2010). 13C–18O isotope signatures and 'clumped isotope thermometry in foraminifera and coccoliths. *Geochimica et cosmochimica acta*, *74*(20), 5697-5717.

Wagner, J. D., Cole, J. E., Beck, J. W., Patchett, P. J., Henderson, G. M., & Barnett, H. R. (2010). Moisture variability in the southwestern United States linked to abrupt glacial climate change. *Nature Geoscience*, *3*(2), 110.